Current Drug Delivery, 2020, *17*, 362-374

PERSPECTIVE

Physicochemical Considerations of Tumor Selective Drug Delivery and Activity Confinement with Particular Reference to 1,2-Bis(Sulfonyl)-1-Alkylhydrazines Delivery

Philip Penketh[1,*], Hugh Williamson[2] and Krishnamurthy Shyam[1]

[1]*Department of Pharmacology, Yale University School of Medicine, New Haven, CT 06520, USA;* [2]*BP Exploration, Chertsey Road, Sunbury-on-Thames, Middlesex, TW16 7LN, UK*

ARTICLE HISTORY

Received: August 15, 2019
Revised: October 21, 2019
Accepted: March 12, 2020

DOI:
10.2174/1567201817666200427215044

Abstract: Hypoxic tumor cell sub-populations are highly resistant to radiotherapy and their presence frequently causes disease recurrence and death. Here, we described the physicochemical properties required to develop superior tumor-targeted hypoxia-activated modular prodrugs that liberate extremely short-lived bis(sulfonyl)hydrazines (BSHs) as reactive cytotoxins, thereby precisely focusing cytotoxic stress on these radio-resistant hypoxic sub-populations. Therefore, cytotoxic stress will be focused on radiation resistant areas and thus strongly synergizing with radiotherapy.

Keywords: Hypoxic tumor cell, bis(sulfonyl)hydrazines (BSHs), cytotoxic stress, hypoxic sub-populations, radiotherapy, hypoxic sub-populations.

1. INTRODUCTION

Recently there has been considerable expansion in the types of therapies available to treat cancers, ranging from immunotherapy to nutraceuticals [1-3]. However, chemotherapy is likely to remain, in the near future, a dominant therapeutic strategy for the treatment of many cancers. Chemotherapy can be improved to largely confine its action to tumors while sparing healthy tissue. In addition, it possesses an inherently lower cost of therapy. The 1,2-bis(sulfonyl)-1-alkylhydrazines (BSH) possess a unique combination of favorable properties that make them ideal chemotherapeutic cytotoxins for selective targeting tumors. We have been particularly interested in the targeting of hypoxic radiation resistant microenvironment, and this perspective will be focused primarily on this strategy. However, BSH can be engineered to be released from prodrug forms under a wide range of conditions by a variety of enzymes or target specific microenvironmental conditions. Thus BSH prodrug forms that are accumulated due to the EPR effect (enhanced permeability and retention effect) could be easily engineered to release BSHs. The highly tunable half-life of BSHs enables the effective confinement of their activity to within close proximity of their site of liberation from the prodrug form. The EPR effect arises because most solid tumors have abnormally large gaps between their capillary endothelial cells, permitting large scale extravasation and retention of macromolecules and macromolecular prodrugs [4]. The EPR effect is not seen in normal healthy tissues. Thus short-lived cytotoxic BSHs could be liberated from prodrug forms in a range of target cells and microenvironments.

2. HYPOXIA AS A THERAPEUTIC TARGET

In normal tissue, mean intercapillary distances (ICDs) are ~ 80 μm thus, most cells reside ≤ 40 μm from a functional capillary [4, 5]; but in tumor tissues mean functional ICDs > 300 μm have been reported [5]. The metabolism of O_2 is higher than all other nutrients, but its free concentrations within capillaries are low (15-40 μM). Thus, O_2 has an unusually short diffusion range within tissues of < 100 μm [6, 7]. This range is insufficient to cope with the atypical microvasculature of tumors creating Hypoxic Tumor Regions (HTRs) [8, 9]. These HTRs are interspersed on a microscopic scale between relatively normoxic regions lying adjacent to functional capillaries. Although HTRs (0-5 μM O_2) have impaired vascular delivery, access by small molecules that lack the unusual supply/demand limitations of O_2 readily occurs. Thus, glucose, present at more than 200-fold greater concentrations than O_2, is not limiting and can sustain HTR cells despite their elevated glycolytic rates. HTRs are a major factor in therapy resistance and disease progression, and are a strongly negative prognostic factor [8,12-23] (Fig. **1A**). Radiation can be used to precisely target tumor tissues, but the sensitivity of cells to radiation is greatly diminished in the absence of O_2 (Fig. **1B**), thus HTR cells tend to survive radiotherapy [8, 24]. Additionally, cancer stem cells that represent the clonogenic core of many tumors appear to pref-

*Address correspondence to this author at the Department of Pharmacology, Yale University School of Medicine, New Haven, CT 06520, USA; Tel: 2032309516; E-mail: philip.penketh@gmail.com

1875-5704/20 $65.00+.00

erentially proliferate and reside in HTRs [25]. These, like normal stem cells, are equipped for long term survival possessing high levels of enzymes involved in detoxification and self-maintenance [26], making them more resistant to chemotherapy. Thus, cells in HTRs are more likely to survive radiotherapeutic and chemotherapeutic treatments and cause relapse and patient death (Fig. **1A**). Strategies to deliver a stronger cytotoxic blow to therapy-resistant HTRs are therefore required. Cells within HTRs exhibit considerably more net reduction of xenobiotics containing particular functional groups largely due to decreased back oxidation by O_2 [8, 14] (Fig **2**). Hypoxia selective net reduction has been successfully exploited in the development of nitroheterocyclic antibiotics (*e.g.*, metronidazole used to treat anaerobic infections) and HTR imaging agents. Upon reductive activation, HTR imaging agents react extremely rapidly with intracellular thiol groups trapping the label close to the activation site [27-29] (Fig. **2**). HTR imaging agents serve as a convincing proof of principle for HTR penetration, and HTR selective agent activation. Several groups have tried to use this phenomenon to produce Hypoxically Activated Prodrugs (HAPs) that selectively liberate therapeutic agents from inactive prodrugs forms in HTRs, thus exposing therapy-resistant cells to active agent while largely sparing normal tissue cells. While the basic principles involved are simple and proven, in practice, the localization of therapeutic quantities of active agent in HTRs is complex, and requires the precise tuning/matching of the properties of the prodrug and the liberated active agent. Prior efforts by several groups resulted in only modest success, largely because of the presence of one or more of the following problems:

A) Facile/rapid activation under mildly hypoxic conditions endowing the agent with O_2 like HTR penetration, and causing agent exhaustion prior to reaching distal HTRs [30, 31]. B) High hydrophilicity slowing HTR penetration and

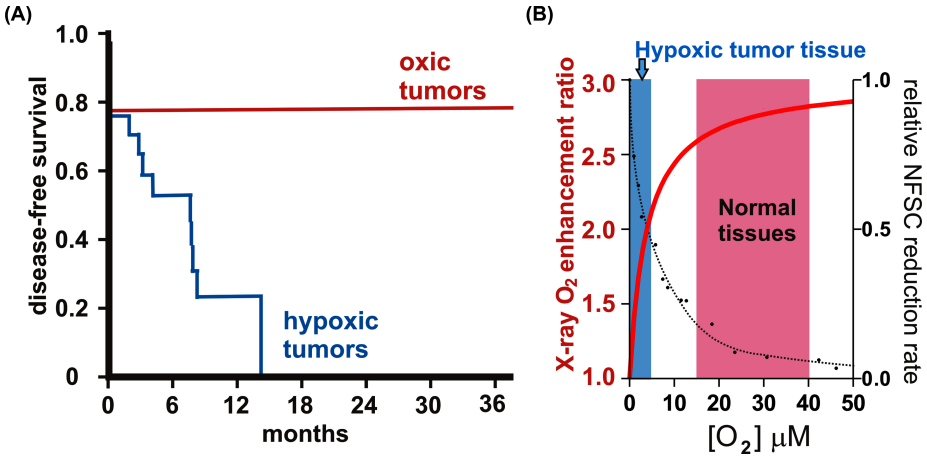

Fig (1). Effects of tumor oxygenation on patient disease-free survival, and O_2 concentration on the cytotoxic actions of X-rays and nitrofurazone reduction. **A**: Kaplan-Meier plot of patients with head and neck carcinoma undergoing radiotherapy. Oxic tumors (mean > 2.8 µM O_2) show superior prognosis to hypoxic tumors (mean < 2.8 µM O_2) [7]. **B**: Comparison of the O_2 concentration dependencies of X-ray cytotoxicity, and the relative reduction rate of the antibiotic nitrofurazone (NFSC) by cytochrome p450 reductase [8], both half-maximal effects occur at ~ 4 µM O_2, but with the O_2 concentration acting in opposite directions.

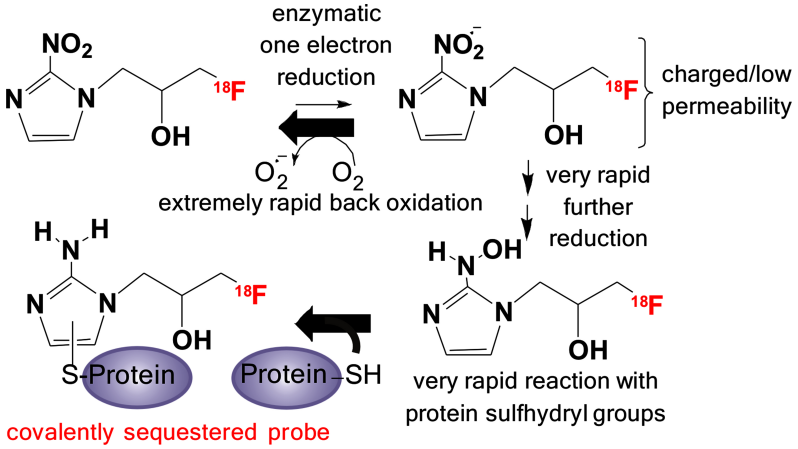

Fig (2). Hypoxia selective binding of fluoromisonidazole. Two factors are key to the effectiveness of fluoromisonidazole as a hypoxic region imaging agent, [1] the extremely rapid back oxidation of the initially one electron reduced agent by O_2 (this imparts [O_2] sensitivity), [2] the confinement and/or rapidity of subsequent reaction steps culminating in the reaction with impermeable biomolecules (this localizes the label within close proximity to its initial site of reduction). The latter process involves multiple pathways, only one of which is illustrated above.

worsening type (A) problems (diffusion within tissues is dependent upon hydrophobicity) [12, 32]. C) Unrestrained escape of the targeted active agent resulting in the attenuation of the HTR focus [33]. D) Low prodrug/active agent structure-activity flexibility preventing flaw(s) correction.

Tirapazamine like agents, for example, have little capacity for tuning either their overly rapid rate of reductive activation or subsequent hasty cytotoxic reaction. If the latter step could be easily slowed, it could impart sufficient bystander action to allow its activity to reach distal HTR and correct for the reductive activation rate flaw and *vice versa*. Agents like Evofosfamide (TH-302) have a near optimal and relatively tunable reduction potential/activation rate, but the liberated cytotoxin (an isophosphoramide mustard) has very modest tunability of its overly long half-life which will attenuate its hypoxic focus in *in vivo* situations. However, the BSHs, which were pioneered in the laboratory of the late Alan C. Sartorelli, are uniquely tunable possessing a combination of properties that allow these cytotoxic warheads to be readily matched to reductive triggers circumventing such concerns.

1) BSHs are readily latentiated as highly stable inactive prodrug forms (Fig **3** panel A) yet are excellent leaving groups, aiding their near instantaneous release from activated HAPs [33].

2) BSHs have short, but widely tunable and predictable half-lives that can be used to constrain the spatial delivery of cytotoxic stress to within a defined range encompassing anticipated optimal values [33, 34].

3) Free BSH warheads are weak acids with pKa values close to neutrality favoring their pH biased entry/concentration within solid tumor cells [33, 34] and slowing their escape from these tissues (tumor cells possess large and inverted trans plasma membrane pH gradients). The opposite is true for weakly basic agents (*e.g.*, doxorubicin) muting their tumor tissue selectivity [35].

4) O^6-methylguanine-DNA methyltransferase (MGMT), the protein primarily responsible for BSH resistance, can provide a strong yet limited 'toxicity threshold', allowing the tolerance of leakage and background non-specific activation [36]. However, the limited/titratable MGMT protection threshold (MGMT is a suicide protein repairing only one lesion per molecule) can be overwhelmed by preferential BSH delivery [36-38]. Additionally, the presence of MGMT deficient tumors in 5-20% of patients (dependent upon the tumor type) may permit the pre-selection of patients likely to exhibit exceptional responses [38-40]. Furthermore, MGMT may be amenable to tumor-selective modulation in solid tumors preferentially sensitizing them to BSHs [33, 41].

5) Chloroethylating BSHs do not cause rapid cell death or induce apoptosis at cidal concentrations [42]. Ex-

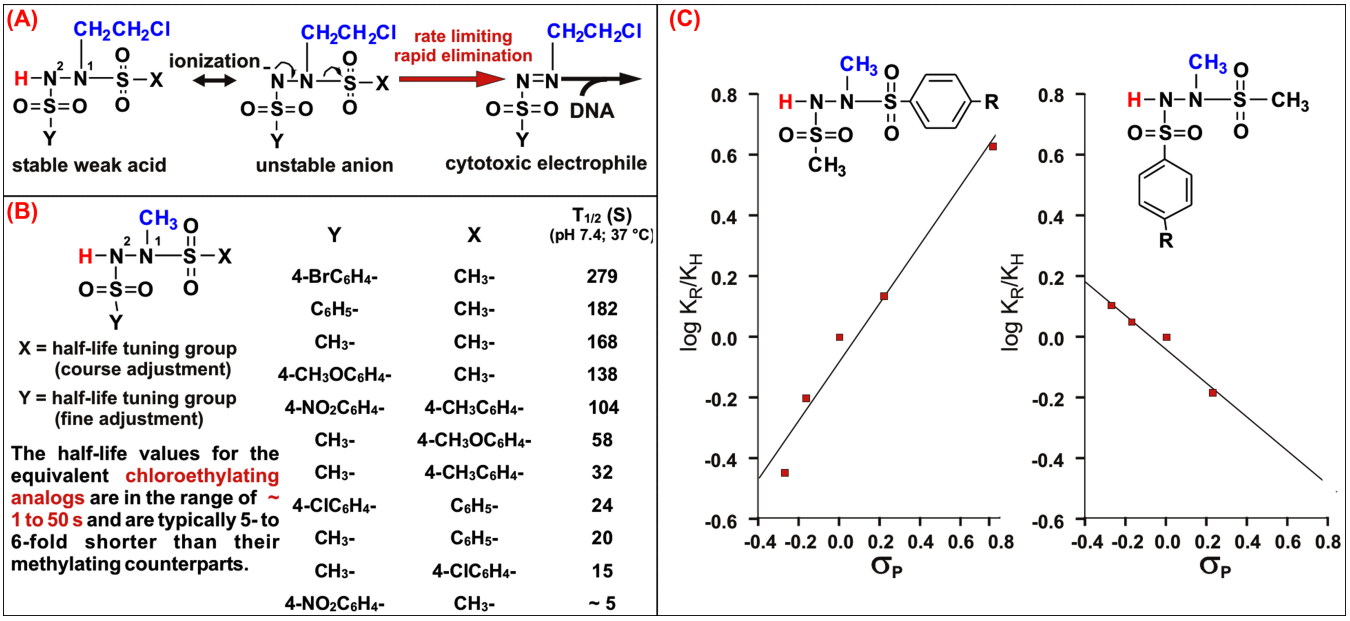

Fig. (3). BSH warhead structure half-life relationships. **A**: Chloroethylating (and methylating) BSHs are very weak stable acids with pKa values close to neutrality, ionization results in the formation of an unstable anion which undergoes a rapid but rate limiting elimination reaction. Replacement of the N-2 proton indicated in red (H) with a hypoxically cleavable masking group blocks decomposition and generates a HAP. **B**: BSHs with half-lives ranging from seconds to minutes have been synthesized. The effects of different substituents in the N-1 and N-2 positions on the half-life values at 37 °C and pH 7.4 for methylating analogs are shown. The 5 to 6-fold shorter-lived chloroethylating analogs are preferred as cytotoxic warheads since they are about one log more potent, and thus require the delivery of less agents. **C**: A Hammett analysis of the effects of various para-substituents (shown in panel 'B') in the benzenesulfonyl moieties attached to N-1 and N-2 on the first-order decomposition rate constants gave linear plots. These N-1 and N-2 substitutions act like coarse and fine half-life adjustments, respectively. This enables the design of BSHs with accurately predetermined half-life values over a wide range.

posed cells stop dividing but continue to increase in size, and slowly die off over an extended period, often lasting more than a week. During this protracted cell death period, these cells are recorded as live by assays based on metabolic reductive capacity, but are not registered by assays dependent upon clonal replication [33]. This metabolically active cell death makes BSHs particularly attractive as HAP delivered cytotoxins as activation will continue, despite the lethal exposure of the activating cell. A cytotoxin that rapidly killed the activating cell would be unsuitable for exploiting the bystander effect, since this would quickly shut down the intra-tumor hypoxic BSH liberating cells.

6) Exhibit outstanding activity in several tumor models, even in simple non-targeted prodrug forms [33].

3. MODULAR PRODRUG STRUCTURE

Modular prodrugs incorporating BSH warheads and nitrobenzylcarbamate hypoxia triggers are readily synthesized. These prodrugs allow the independent tuning of the activation rate/oxygen sensitivity of the trigger, and the precise tuning of the cytotoxic BSH half-life (major factor controlling BSH activity radius). The half-life tunability (Fig. **3**) allows the warhead to mimic the short-lived electrophiles generated by HTR imaging agents resulting in the HTR confinement required for their function. The use of nitrobenzylcarbamate hypoxic trigger results in a hydrophobic prodrug that transitions to a hydrophilic active agent favoring tumor penetration by the prodrug form but hinders the escape of the liberated BSH (Fig **4**). This is an ideal transition for HAPs used in combination with radiotherapy according to recent pharmacokinetic/pharmacodynamics models [12, 32].

To function effectively in conjunction with radiotherapy, HAP physicochemical parameters need to be tuned so that the cytotoxic stress is precisely focused upon the HTR that results in significant radioresistance. A lead agent 1,2-bis(methylsulfonyl)-1-(2-chloroethyl)-2-[[1-(4-nitrophenyl) ethoxy]carbonyl]hydrazine (KS119), despite liberating a BSH (90CE, 1,2-bis(methylsulfonyl)-1-(2-chloroethyl)hydrazine) with an overly long half-life (~30 seconds) based on modeling studies (see later), still exhibited a greater *in vivo* enhancement of the effects of radiation that is seen with most radiation/drug combinations. This exceptional activity resulted in KS119 and closely related more soluble analog (KS119W) being short-listed for clinical development [33]. Unfortunately, neither KS119 nor KS119W were ever clinically evaluated owing to the financial failure of the developing company [33]. However, this interest underscores the clinical potential of this HAP class. The optimization of both the nitrobenzylcarbamate hypoxia trigger and BSH should enable the design and synthesis of HAPs with significantly superior performance to that of KS119/KS119W and other HAP designs. The high frequency of therapeutic limitations arising from HTRs means that such agents would be ex-

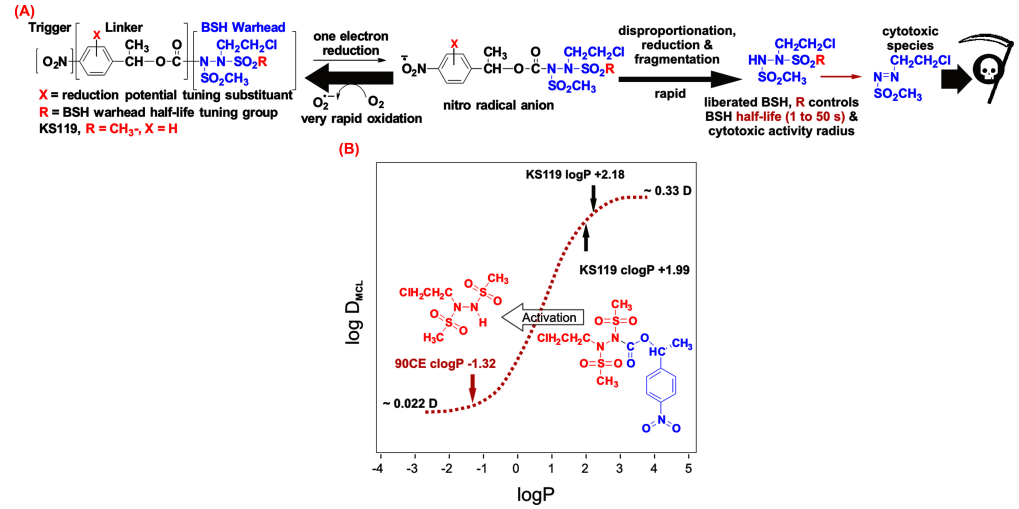

Fig (4). HAP structure, activation mechanism, and hydrophobic switch. (**A**) BSH warhead liberation occurs selectively under hypoxia due to a large reduction in the rate of the O_2 dependent back oxidation reaction. The BSH liberation reaction sequence is then anticipated to occur largely within the activating cell because the radical anions are charged (low permeability) [44]; and the subsequent steps are very rapid [30,41]. Hence, activating cells are likely to approximate to 'point sources' of cell permeable BSHs. Einstein's diffusion approximation equation $t \approx (\Delta x)^2/2D$ gives the average time (t), it takes a molecule to diffuse a distance (Δx) in one dimension, where D = the diffusion coefficient [45]. Since the required diffusion time increases with the square of the distance, diffusion is rapid over very short distances but slows disproportionately as the distance increases. The half-life of the BSH limits travel time, essentially confining the cytotoxicity to a sphere around a point source of constant BSH generation. (**B**) The diffusion coefficient of small molecules through multi-cell layers (DMCL) unlike that in pure aqueous solutions (D) is highly dependent upon the molecule's hydrophobicity and exhibits a sigmodial relationship with respect to logP [29]. Hydrophilic molecules have DMCL values ~ 40 to 50-fold lower than that in pure water, whereas hydrophobic molecules have values only 3 to 5-fold lower [29]. The HAP KS119 has a logP of +2.18 (calculated logP (clogP) +1.99), suggesting it should readily penetrate tissues, whereas the relatively hydrophilic active 'warhead' liberated on reductive activation has a clogP of -1.32 that should impede its escape. This switch in hydrophobicity is expected to aid in the retention of HTR targeted BSH warheads by slowing their escape *via* diffusion, thus giving them more time to react and exert their cytotoxic action.

pected to have extensive clinical utility. Moreover, HAPs with the tight activity zones possible with BSH warheads are also likely to be of utility in approaches where prodrug-activating enzymes are selectively delivered to or expressed in tumor tissues using modified macrophages, bacteria, genetic, or nanoparticle approaches. The use of bacterial two electron nitroreductases (not present in mammalian cells) would allow nitrobenzylcarbamate based prodrugs to be selectively activated in tumor tissues in an O_2 concentration independent manner, expanding their utility beyond tumors containing HTRs. Bioreductively or otherwise activated BSH-prodrugs with adjustable bystander kill would mesh well with these developing anticancer strategies that function as tumor targeted 'molecular-trucks' as these approaches need to ultimately generate a tumor confined effect, rather than selectively deliver something that then immediately redistributes.

4. HAP STRUCTURE, REDUCTION RATE, O_2 INHIBITION SENSITIVITY, AND OPTIMAL ACTIVITY RADII

Flexible HAPs are composed of three independently tunable primary domains, a trigger region, a linker region and a cytotoxic warhead domain [33, 41, 43-46] (Fig. **4**). The trigger (the O_2 sensing domain) undergoes one electron reduction to form a radical anion by enzymes such as cytochrome P450 reductase [33, 43, 44]. This radical anion is briskly oxidized by O_2 to regenerate the parental HAP under oxic conditions. Thus, further reduction, resulting in linker fragmentation and the release of the warhead, can only occur readily under hypoxic conditions. In an *in vivo* situation, HAPs require a slow initial one electron reduction rate to avoid agent activation prior to full HTR penetration. This sets a functional window for HAP one electron reduction potential. Earlier HAP designs despite exhibiting large hypoxic/oxic activation rate differentials in various cell line suspensions and excelling in several *in vitro* assays [31, 33] failed to deliver in *in vivo* assays. This is because a large fold hypoxic/oxic activation rate differential cannot be manifested as a therapeutic advantage unless the oxic activation rate is low, since there must be sufficient time as to allow the parental HAP to equilibrate with tumor tissue, and for the hypoxic activation to act as a HAP sink. In tissues, the cell densities are more than 100-fold greater than in most *in vitro* experimental conditions. This results in a proportional increase in the rate of HAP metabolism, causing the HAP to be expended prior to reaching even modestly HTRs [30, 31]. Thus, low normoxic activation/metabolism rates are imperative for successful *in vivo* targeting of hypoxic cells. To achieve such low normoxic activation rates at physiological cell densities, HAPs require one electron reduction potentials at pH 7.0 (E^7_1) of < -350 mV. At the other extreme, agents with E^7_1 values < -470 mV are usually not reduced at all by mammalian cells resulting in a loss of O_2 concentration sensitive activation. This sets a functional window for HAP E^7_1 values of between ~ -470 mV up to -350 mV. There is a strong correlation between E^7_1 values and half-wave reduction potentials ($E^7_{1/2}$) [45] for nitroheterocycles and nitrobenzenes; and the corresponding $E^7_{1/2}$ value window versus an Ag/AgCl (saturated KCl) reference electrode is ~ -400 mV up to -280 mV. This entire functional range can easily be encompassed by substituted derivatives nitrobenzene triggers [49]. The HAP's one electron reduction potential has an additional important consequence in that it, for the most part, determines the rate of the restitution reaction (that is the rate of reaction of the initial radical anion product with O_2) [50]. The lower the one electron reduction potential is, the faster the restitution rate. The relative rate of the restitution reaction in competition with its loss *via* further reduction/dismutation *etc*. (net activation pathway) determines the HAP's sensitivity for O_2 concentration inhibition of activation. While the restitution reaction rate is not the sole determinant of O_2 sensitivity, lower reduction potentials tend to result in a greater sensitivity to O_2 concentration. A value K_{O2} can be defined as the O_2 concentration that inhibits HAP activation by 50% of its anoxic rate under test conditions [8, 50]. Ideally, the KO_2 value should be sufficiently lower than normal physiological O_2 levels to minimize toxicity to normal cells, while resulting in therapeutic agent delivery to hypoxic tumor regions that mirror the O_2 concentration dependency of radiation sensitivity, that is exposing the most hypoxic/radiation resistant cells to the greatest pharmacological cytotoxic stress. Therefore, a K_{O2} value of ~ 4 μM would appear to be preferable if judged solely on this criterion. The reductively activated antibiotic nitrofurazone exhibits a K_{O2} that closely matches the half maximal radiation sensitizing O_2 concentration (Fig. **1B**) [11]. Radiation, coupled with a HAP with a K_{O2} of ~ 4 μM, could theoretically level cell kill across relevant degrees of oxygenation if its cytotoxic actions remained largely confined to the activating cells (~ 10 μm radius). However, if the cytotoxic activity can escape the activating cells into more oxygenated areas (or reach capillaries and get fast tracked away), the resulting redistribution would eradicate the appropriate hypoxic proportionality of its cytotoxicity, and result in a cubic dilution of the desired cytotoxic stress on the target cells with the expanding sphere of activity. To exhibit near cellular confinement, the activated agent/warhead would require an extremely short half-life (most likely < 0.5 s, even for a low permeability polar molecule) or be impermeable. These parameters (HAP K_{O2} ~ 4 μM, coupled with a sufficiently slow reduction rate, and post-activation $t_{1/2}$ < 0.5 s) are likely to be very difficult to achieve. However, there are several reasons why picking agents with more readily attainable, K_{O2} [8, 50, 51] and half-life values would be better. Harder to reduce agents (those with more negative one electron reduction potentials and generally lower K_{O2} values) tend to exhibit lower toxicities to normoxic tissues and better hypoxic/oxic selectivity, in addition to gaining a desirable slower initiating one electron reduction rate that permits better tumor penetration/equilibration [30, 31]. To match this more extreme hypoxia activation preference, such agents would benefit from liberating a longer-lived cytotoxic BSH (again within a more easily attainable range) to impart a bystander kill to their immediately flanking less hypoxic neighbors. The liberation of a short-lived cytotoxin in strongly hypoxic regions with a cytotoxic activity radius of only ~ 30 - 50 μm would easily expand its reach to encompass bordering, more mildly hypoxic/radiation resistant regions. This is because the diffusion range of O_2 is < 100 μm, and a relatively linear O_2 concentration gradient from ~ 15 - 40 μM near capillaries to anoxia occurs over this span [42] and radioresistance would largely increase over the lower one third of this O_2 concen-

tration range (Fig. **1B**). Hence a progressive attenuation of radiation dependent tumor cell kill occurs beyond ~ 70 μm from capillaries (~ 30 μm from the anoxic border) (Fig. **5**). A cytotoxic activity radius much greater than ~ 30 - 50 μm would be increasingly detrimental to the HAP's performance because as the bystander kill radius is expanded, there is a large cubic dilution in the cytotoxic stress delivered per unit volume, coupled with the loss of significant amounts of active cytotoxin to the capillary networks, where it is 'fast tracked' for systemic distribution. Thus the activated HAP should have a < 10 to 50 μm activity range depending upon the prodrugs K_{O2} value (4 to < 1 μM). It should be noted that the K_{O2} value is not a threshold and that increased activation is apparent long before the K_{O2} value is reached (Fig. **1B**, Fig. **5**), and preferential activation will still occur (at lower rates) in more mildly radiation resistant regions even if the K_{O2} value is considerably < 4 μM. However, activation at lower rates, especially by small clusters of marginally hypoxic cells, would strongly benefit from an activity radius that prevents the excessive loss of cytotoxic activity into surrounding areas. This would occur in areas of intermediate ICDs where cells with somewhat increased radiation resistance may not border on large hypoxic, strongly HAP activating regions with a robust bystander kill effect (see later). Thus, the largest BSH activity radius to optimally augment radiotherapy is likely to be much smaller than those possessed by KS119/KS119W, which liberate 90CE (half-life ~30 s) (Fig. **5**). Extremely short BSH activity ranges (< 10 μm) that confine the cytotoxicity to individual activating cells may have a greater tendency to lead to resistance in a similar manner to that observed with molecularly targeted agents by selecting for low sensitivity/low activating individual cells. However, with longer activity range warheads, a cell's experienced cytotoxic stress is not greatly influenced by its own HAP activation (see later modeling).

5. BSH HALF-LIFE AND MULTI-CELL LAYER DIFFUSION COEFFICIENT (D_{MCL}) DETERMINE THE ACTIVITY RADIUS

The liberation of the BSH warhead subsequent to the initiating one electron reduction of KS119 under hypoxic conditions (Fig. **4A**) likely occurs largely within the activating cell for the following reasons: - (a) Nitrobenzene radical anions pKa values are between 2.2 to 3.9 [47] and are therefore fully charged at cellular pH values and of low membrane permeability. (b) The subsequent stepwise reduction to give the unstable hydroxylamino and amino products is very rapid. This process is presently not fully understood but appears to involve disproportionation and a series of radical reactions/one electron reductions [52]. Thus, cytochrome P450 reductase (and xanthine/xanthine oxidase) reduction of nitrobenzene (a model of the nitrobenzylcarbamate trigger/linker) results in mixtures of untouched starting material and hydroxylamino and amino products, but no intermediately reduced species are detected [41]. (c) When KS119 is 'flash reduced' (Zn/EDTA), the kinetics of the loss in DNA cross-linking capacity on aging match the half-life of 90CE ($t_{1/2}$ ~ 30 s) (the liberated BSH) [44]. Therefore, the fragmentation of the unstable reduced form(s) to liberate 90CE is much faster than the decomposition of the liberated BSH (90CE) itself. Thus individual activating cells likely approximate to 'point sources' of short-lived BSH. Therefore, the half-life of the liberated BSH and its tissue/Multi-Cell Layer (MCL) diffusion coefficient D_{MCL} will essentially determine the activity radius of the activated HAP. Of these factors, the BSH half-life is likely to be the largest determinant since it is tunable over at least a 50-fold range (Fig. **3**). The D_{MCL} of a molecule is a function of both its molecular size and partition coefficient [12], and since the molecular weight range of the BSHs of interest is relatively small, this factor will have little overall effect. Large differentials in

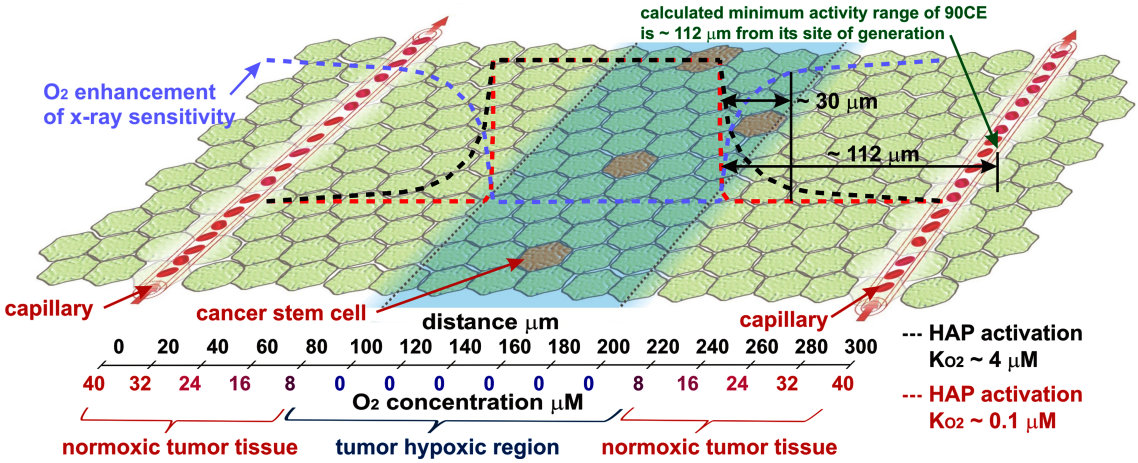

Fig. (5). Graphical illustration of the relationship between ICD, O_2 concentration, O_2 enhancement of X-ray sensitivity, and the activation of HAPs with K_{O2} values of 0.1 and 4 μM in a section of tumor tissue with an ICD of ~ 300 μm. A linear O_2 concentration gradient down to zero over 100 μm is assumed. Since the O_2 enhancement of X-ray sensitivity occurs over a narrow (~ 0-10 μM) O_2 concentration range, X-ray resistance increases progressively beginning at ~ 70 μm from capillaries and extending through the anoxic region. If HAP activation was essentially restricted to the anoxic region (very low K_{O2} value) a bystander kill range of only about ~ 30 μm would be required to extend its reach to cover cells with significantly increase radioresistance, and an agent with a K_{O2} value of 4 μM would require little or no bystander kill to level cell kill over a 0-10 μM O_2 concentration range. The calculated minimum activity range of 90CE (point of ~ 90% activity dissipation) is ~ 112 μm from its point of generation, this is overly long even when generated by a HAP with K_{O2} of ~ 0.1 μM. The predominant hypoxic location of cancer stem cells is also indicated.

partition coefficient (2.5 logs) can result in equivalently sized molecules differing by as much as 15-fold in their D_{MCL} [12]. However, BSHs have an acidic N-2 proton with pKa values a little below neutrality (Fig. **3**) and this tends to reduce their logP and place them towards the lower permeability end of the sigmoidal log D_{MCL} versus logP curve (Fig. **4**).

6. KS119 CHARACTERISTICS AND FLAWS

Despite the fact that KS119 and its water soluble analog KS119W exhibited remarkable performances in some *in vitro* and *in vivo* assays (Fig. **6**) [44, 53], they have considerable potential for improvement as several of their key physicochemical parameters appear to be non-optimal. This is in part due to the fact that some *in vitro* assays fail to adequately test several critical factors. The spectacular *in vitro* > 5-log hypoxic/oxic cell kill selectivity of KS119 our prototype HAP [29] is likely difficult to exceed. However, this type of assay (Fig. **6** Panel **A**) is an inaccurate representation of KS119's *in vivo* hypoxic/oxic discrimination (Fig. **6** Panel **B**) because it essentially neglects the importance of both the K_{O2} value and the cytotoxic BSH activity range. In this assay, there are only two oxygen values, normoxia and near anoxia, so virtually any K_{O2} value would function equivalently. Additionally, the long incubation (2 h) in a closed system is blind to the weaknesses of longer-lived BSHs since they cannot be lost to other cell populations (the normoxic control flask), and there is no reference to gauge warhead potency loss due to escape from activating cells and reaction in the surrounding incubation media. Thus, optimized HAPs need evaluation based on direct measurements of these parameters and the use of the more astute *in vitro*/*in vivo* assay (Fig **6**. Panel **B**). Our recent studies concerning the modeled activity radius of BSH warheads, KS119/KS119W stability, activation rates, and solubility have pointed the way to design significantly superior KS119/KS119W analogs.

7. CORRELATING BSH HALF-LIFE WITH CYTOTOXIC ACTIVITY RADIUS/RANGE

If we assume that a permeable, relatively slow metabolized HAP is uniformly distributed throughout a tumor, and that a hypoxic cell by slowly activating this agent acts as a 'point source' of short-lived BSHs with a defined half-life, then it can be shown by applying Fick's second law of diffusion that the steady-state concentration of BSH at a distance Δx from the point source of continuous generation can be described by the below equation [54].

$$[BSH]_X = [BSH]_0 \exp[(-1n\ 2)(\Delta x) / \sqrt{2D_{MCL}t_{1/2}}]$$

Where, $[BSH]_X$ = the concentration of BSH at a distance Δx from the point source; $[BSH]_0$ = the concentration of BSH at the point source of constant generation; D_{MCL} = the multi-cell layer diffusion coefficient of the BSH; and $t_{1/2}$ = the half-life of the BSH. This modeling approach has been previously used to investigate the range of action of the short-lived signaling molecule nitric oxide (NO) from NO generating cells [55]. Diffusion coefficients in free aqueous solutions at 37°C can be predicted (with reasonable accuracy) using the relationship described by Hobbie [56], where the aqueous diffusion coefficient is a function of molecular size and temperature. For 90CE, this value calculates to be 913 $\mu m^2 s^{-1}$ and very similar values (within 20%) are calculated for other BSHs. Using the simple methodology described by Crooks [57] and acidified solutions (pH ≤ 3.0 to block BSH activation/decomposition), these diffusion coefficients could be easily measured directly. Diffusion through cells and tissues is generally a slower process because of a number of factors, including the need to traverse multiple membranes, cytoplasmic viscosity, *etc*.

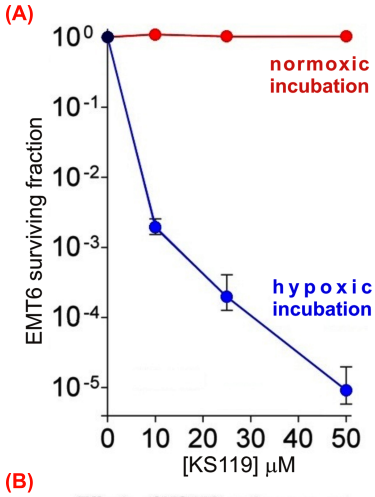

(B)

Effects of KS119 and x-rays on EMT6 tumors in BALB/c mice

Treatment	Surviving fraction
None	1.00
15 Gy x-ray	0.0380 ± 0.007
60 mg/kg KS119	0.83 ± 0.18
60 mg/kg KS119 + 15 Gy x-ray	0.0070 ± 0.0001

Fig (6). KS119 *in vitro* and *in vivo* hypoxia selective cytotoxicity. **A**: KS119 demonstrates a very strong *in vitro* hypoxia selective toxicity towards EMT6 cells, with 50 μM KS119 producing ~ 5 logs of cell kill under hypoxia in 2 h; whereas no discernable normoxic cell kill is observed. **B**: KS119 demonstrates *in vivo* enhancement of the effects of radiation. The surviving fraction of EMT6 cells isolated from established tumors (150 mm^3) in BALB/c mice post *in vivo* treatments with KS119 and X-rays combinations was measured. The x-ray dose was sufficient to virtually eradicate the oxic fraction. Thus the cells that survive this exposure (~ 4%) represent the hypoxic fraction. KS119 alone results in little tumor cell kill, but the combined treatment results in only a very small surviving fraction. These results are consistent with KS119 preferentially targeting hypoxic tumor regions, coupled with the bystander kill of bordering normoxic regions, and a small proportion of cells escaping both modalities. Theoretical modeling of 90CE delivery provides a possible explanation for how aerobic cell populations closely associated with hypoxic regions areas can be heavily targeted and yet some very small hypoxic cell populations can evade killing, and drug design changes to remedy this flaw.

Thus, diffusion through Multi-Cell Layers (MCLs), unlike that in purely aqueous media, is strongly influenced by a molecule's partition coefficient [9]. Small lipophilic molecules with logP values > ~ +1.5 traverse cell layers relatively rapidly, at up to $1/3^{rd}$ of their aqueous solution diffusion coefficient controlled rate, whereas small relatively hydrophilic molecules with logP values < ~ -1.0 traverse cell layers a

further 15-fold slower (45-fold slower than their equivalent aqueous solution diffusion rate). Either side of this -1.0 to +1.5 logP range, little change in the MCL diffusion coefficient (D_{MCL}) occurs with respect to further decreases or increases in lipophilicity [12]. The very short half-lives of BSHs (the ones we are interested in are all ≤ 30 s) at physiological temperature and pH prevent the direct measurement of their D_{MCL} values. However, since the calculated logP (clogP) values for 90CE (Fig. **4**) and closely related BSHs place them at the hydrophilic end of the sigmoidal step (clogP ~ -1.0), a value of ~20 $\mu m^2 s^{-1}$ would seem to represent a reasonable minimum estimate for their D_{MCL} values. The use of closely related but stable BSH analogues may allow a more precise experimental estimation of D_{MCL} values; but this minimum D_{MCL} value is a useful starting point for initial approximations of the minimum cytotoxic activity range of a point source of 90CE and related BSHs. A BSH D_{MCL} value of ~20 $\mu m^2 s^{-1}$ requires a half-life of ≤ 0.5 seconds to confine the majority of the cytotoxic action to the source cell, assuming an average cell is approximately a 20 µm sphere (Fig. **7**), and a BSH such as 90CE with a half-life of ~ 30 s appears to have too large a zone of activity to be close to optimal for precisely targeting hypoxic regions, likely resulting in unnecessary loss of material from the hypoxic target and into the capillary network (Fig. **5**). Each time the radius of the activity zone is doubled, there is an 8-fold drop in the cytotoxic stress experienced by a single activating cell. However, when the zone of activity has a large radius, as with 90CE, the additive effect of co-activating neighbors can be very significant, and with large 3-dimensional clusters, the bystander effect can be magnified several hundred fold (Fig. **8**). These effects would result in very small isolated hypoxic cell clusters receiving much smaller non-lethal BSH exposures while large clusters of hypoxic cells and their flanking oxic neighbors received lethal doses. These predictions match the experimental observations in our *in vivo* treatment of EMT6 tumors with KS119 and x-radiation (Fig. **6** panel **B**), where KS119 alone killed in excess of the radiation resistant hypoxic fraction, yet in the combined treatment, a small fraction escapes the cidal effects of both modalities. A BSH with a half-life between 2-8 s would be expected to resolve such problems. It is realized that other factors such as dynamic hypoxic regions arising from temporal variations in blood flow [58] (oxic during KS119 treatment, but hypoxic during radiation exposure) could provide alternative explanations, especially if the biological half-life of the HAP (in this case KS119) was short. Our modeling of the activity zones of BSHs strongly suggests that the BSH must possess a very much shorter $t_{1/2}$ value than used in previous designs to function optimally in

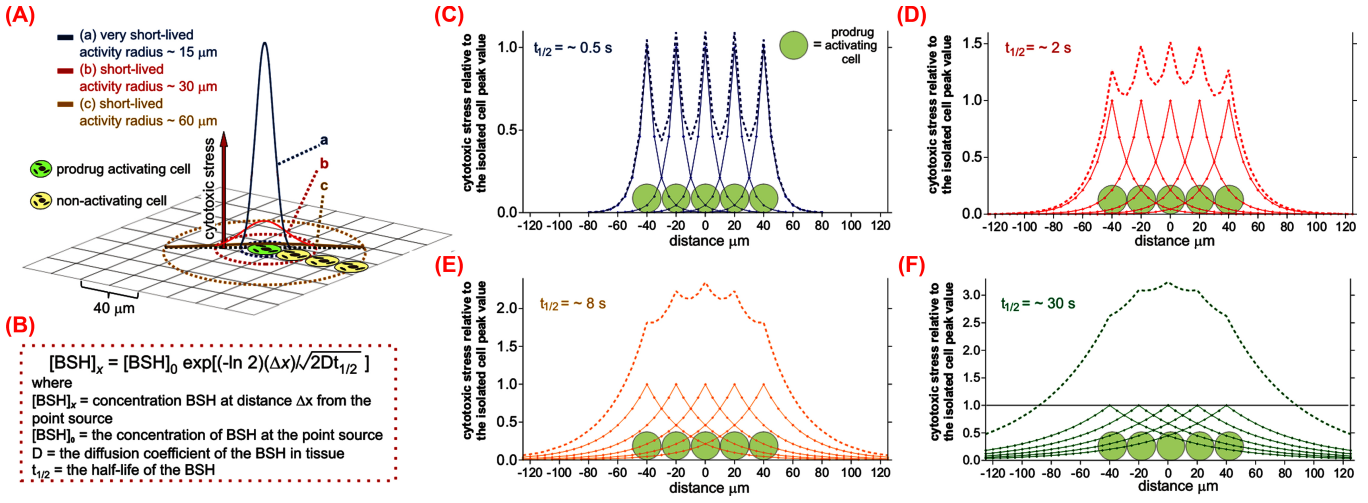

Fig. (7). HAP warhead half-life, activity radii, bystander effects and biological implications. **A**: Visual depiction of a HAP activating cell generating BSH warheads with various activity radii. To double the activity radius requires a 4-fold increase in half-life. The peak height is approximately proportional to the cytotoxic activity, with equivalent quantities of BSH reacting in spheres with volumes in the ratio of 1 : 8 : 64. Thus, long-lived BSHs have lower potencies when considering a single isolated activating cell but longer range bystander effects. **B**: If a hypoxic cell acts as a 'point source' of constant production of short-lived BSHs, it can be shown by applying Fick's second law of diffusion that the steady-state concentration of BSH (cytotoxic stress) at a distance Δx can be described by the equation in panel B [45]. This modeling approach has been previously used to investigate the range of action of the short-lived signaling molecules [46]. Graphs C to F represent the calculated effects using the relationship in B of five 20 µm diameter activating cells in a linear conformation on the cytotoxic stress, a tissue diffusion coefficient (estimate based on typical BSH MW and cLogP) of 20 $\mu m^2 s^{-1}$ and half-lives of ~ 0.5 s, 2 s, 8 s and 30 s were used, respectively. The activity due to each cell and the combined activity are shown with solid and dashed lines, respectively. The Y-axes compare the relative cytotoxic stress to the peak value generated by an isolated cell and are not equivalent between graphs **C** to **E**. A half-life of < 0.5 s essentially confines the cytotoxic stress to the activating cell, as the half-life is increased, so is the contribution from neighboring cells towards the total cytotoxicity. **F**: corresponds to 90CE (half-life ~30 s [30]), the 'warhead' used in KS119. These short linear strings are massive understatements of the expected additive effects experienced in large 3-dimensional cell clusters for BSHs possessing large activity radii where 100's of cells can contribute to the aggregate cytotoxicity, increasing it by > 100-fold.

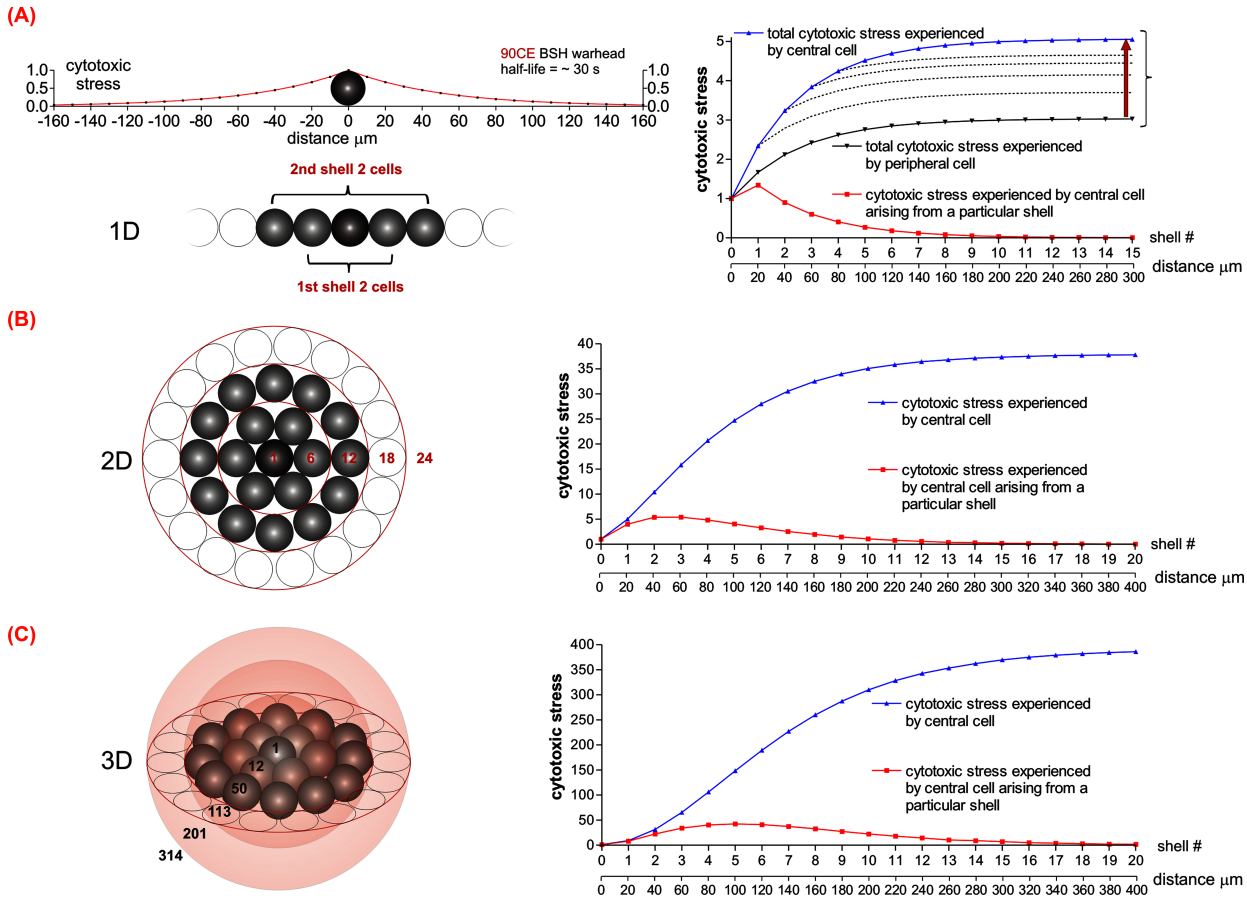

Fig (8). The effects of activating cell community size and conformation on the cytotoxicity experienced by central (and peripheral) cells to intracellularly generated 90CE. **A**: Left: A single 20 μm diameter cell acting as a point source of 90CE, the relative steady-state 90CE concentrations at various distances from the point source are based on a half-life of 30s and a tissue diffusion coefficient of 20 $\mu m^2 s^{-1}$. The point source 90CE concentration has an assigned peak value of 1.0. Right: The cytotoxicity experienced by the central cell of a linear conformation of cells (as shown left) increases with shell number (cells added to either side) and tends to a maximum value of ~ 5-fold that of an isolated cell (1 unit generated internally and ~ 4 units from bystander delivery). A cell at the periphery experiences a maximum value of ~ 3-fold that of an isolated cell (1 unit generated internally and ~ 2 units from bystander delivery). Cells experience an increase in cytotoxic stress (90CE concentration) moving through the peripheral layers towards the center, the dashed curves represent cell depths of 1, 2, 3, and 4 cells inboard of the peripheral cell. **B**: The cytotoxicity derived from the bystander effect is greatly magnified in a two-dimensional layer of cells. Using a loose 'square pack' of spherical cells, the number of neighboring cells in shells 1, 2, 3, and 4 is 6, 12, 18, and 24. This results in a large increase in the bystander effect in terms of magnitude and range. The peak cytotoxic stress tends to a value of ~ 38-fold greater at the center than an isolated activating cell would experience, and now the relatively distal shell # 3 is the greatest contributor to the bystander effect rather than the nearest neighbor shell as in the linear conformation 'A'. **C**: In a three-dimensional configuration, using a simple 'cubic pack' of spherical cells in each shell layer (cells occupy ~ 52% of the volume, likely an underestimate), the number of neighboring cells in each shell increases even more dramatically resulting in the peak cytotoxic stress tending to a value of ~ 390-fold greater at the center than an isolated activating cell would experience, and now the relatively distal shell # 5 is the greatest contributor to the bystander effect experienced by the central cell. In the center of large activating cell clusters, the cytotoxicity experienced would be comparable to an extremely short-lived BSH where it essentially all reacts within the activating cell. A cell positioned on the surface of a large 3-dimensional activating cell cluster could receive > 150-fold times the cytotoxic stress of an isolated activating cell (whether it was an activating cell or not), and this halo of activity would extend well beyond the activating cell cluster, still exceeding a value of 10-fold at ~ 135 μm.

conjunction with radiation, and, in particular, to demonstrate strong activity against small hypoxic cell clusters. A shortening of the BSH $t_{1/2}$ from 30 s (in KS119) to ~ 5 s should increase the cytotoxic stress on individual activating cells ~ 14-fold and still provide a robust bystander effect of sufficient range to reach more mildly hypoxic neighbors, whilst essentially eliminating loss to the capillary networks. A HAP generating a BSH with a $t_{1/2}$ of ~5s would still possess a cell community dependent cell kill that should minimize the selection for non-HAP activating individual cells.

8. THE NITROBENZYLCARBAMATE TRIGGER ADVANTAGE, AND IMPROVED FOURTH SOLUBILIZING DOMAIN DESIGNS

Our KS119 nitrobenzylcarbamate trigger was a modification of an earlier design used in PNBC (1,2-bis(methylsulfonyl)-1-(2-chloroethyl)-2-[(4-nitrobenzyloxy) carbonyl]hydrazine), a closely related agent of lower hypoxic/oxic selectivity [43, 44]. The trigger in PNBC lacks the shielding methyl group on the methylene carbon adjacent

to the linker region (Fig. **9**) and as such, in addition to reductive activation, is subject to S_N2 nucleophilic attack at the methylene carbon (*e.g.*, by glutathione/glutathione-S-transterases *etc*.) [43, 44]. This can result in the release of the warhead in the absence of reduction [40, 56]. The addition of the shielding methyl group in KS119 blocked this mode of activation, and significantly increased the hypoxic/oxic selectivity [43, 44]. In addition to its enhanced resistance to other routes of activation, this trigger type offers relatively simple chemistry, the widest range of reduction potential tuning, and generates a highly desired hydrophobic to hydrophilic transition (when coupled to BSHs) upon activation (Fig. **4**). In the case of KS119, the logP value (~ 2.18) is shifted compared to its liberated BSH (90CE, clogP -1.32) by ~ 3.5. This nicely moves the warhead bearing this trigger from the relatively hydrophilic slowly diffusing side of the -1.0 to +1.5 logP sigmoid step to the rapidly diffusing hydrophobic side in the HAP form. Thus, the HAP form should rapidly diffuse throughout tumor tissue, whereas the 'free' BSH should be relatively retained. HAPs based on the far more polar 2-nitroimadozole triggers do not result in such favorable clogP shifts on activation in either magnitude or appropriate direction. The high hydrophobicity of KS119 comes at the price of limited solubility, which, while still permitting *in vitro* studies, and *in vivo* murine studies using DMSO as a vehicle, would present problems for clinical evaluation. Vion Pharmaceuticals attempted to solve this issue by incorporating a serum phosphatase cleavable phosphate group ortho to the nitro group as a 4th solubilizing domain [33]. The resultant molecule, as expected, was highly soluble, permitting facile formulation. The phosphate group as per design was rapidly cleaved by serum phosphatases to yield the hydroxyl form KS119WOH after intravenous administration (Fig. **9**). However, this design resulted in a new problem since dephosphorylation of KS119W to yield KS119WOH resulted in the generation of a phenolic hydroxyl ortho to a nitro group and was thus at least partially charged at physiological pH due to resonance stabilization (Fig. **9**). This change likely impaired tumor penetration and offsets some of the benefits of enhanced solubility. The net result was a soluble agent, which only performed comparably to KS119 *in vivo/in vitro* models [53]. Additionally, the intrinsic stability of KS119WOH was lower than that of KS119 [45]. A design with a $-CH_2-$ spacer between the phosphate (or a thiophosphate) and the phenyl moiety would retain the high solubility of KS119W, and minimally perturb the hydrophobicity (and stability) of KS119 once the phosphate was cleaved (Fig. **9**). With this refinement, redox potential optimized nitrobenzylcarbamates would be expected to significantly exceed the performances of both these previous trigger domain designs (Fig. **9**).

9. POTENTIAL FOR SYNERGISTIC INTERACTIONS BETWEEN HYPOXIA TARGETED METHYLATING AND CHLOROETHYLATING BSH BASED HAPS

This approach doubly exploits hypoxic targeting using two hypoxia selective synergistic agents, the first to selectively impair MGMT activity (liberating a guanine *O*-6 methylating BSH), the second to exploit this induced deficit with a guanine *O*-6 chloroethylating BSH. The cytotoxic effects of methylation and 2-chloroethylation at guanine *O*-6 differ in important aspects. O^6-methylguanine is rapidly repaired/titrated by MGMT and O^6-methylguanine lesions only persist and result in toxic actions if the number of methylations exceeds the number of MGMT molecules by ~ 5,000 lesions [36, 60]. Thus guanine *O*-6 methylators are of relatively low toxicity, but are superb MGMT depletors. In contrast, O^6-chloroethylguanine undergoes a spontaneous rearrangement to produce the highly lethal G-C ethane cross-link, which cannot be repaired by MGMT [33]. For a cell to survive, a large excess of MGMT molecules relative to the number of chloroethyl lesions is required to produce a repair rate that clears the cross-link precursor lesions before a small

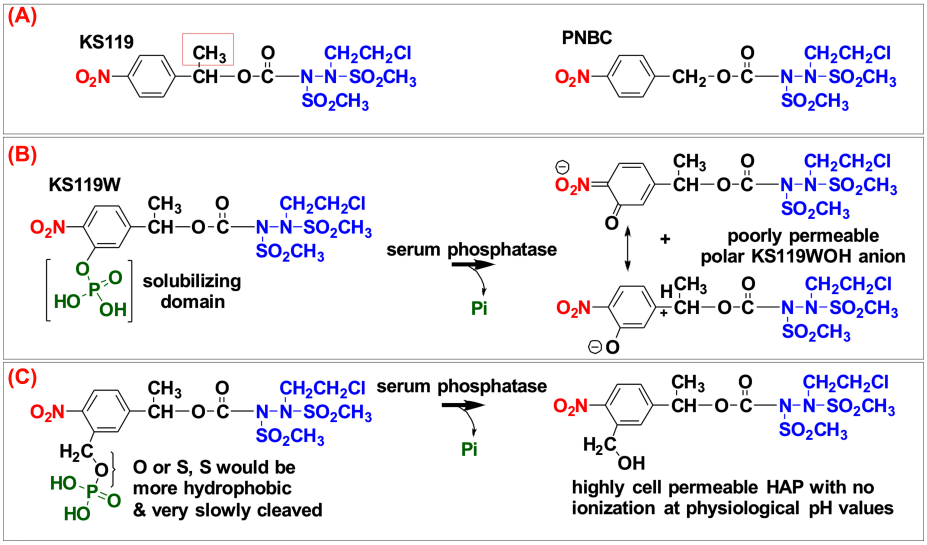

Fig. (9). KS119 analogs. **A**: The structures of KS119 and PNBC. The position of the S_N2 nucleophilic attack blocking methyl group on the methylene carbon in KS119 is indicated by a red box. **B**: The structure of KS119W (the water-soluble KS119 analog) and the removal of the solubilizing phosphate group by serum phosphatase to yield KS119WOH a charged anionic HAP species at physiological pH values. **C**: The structure of a KS119W analog that circumvents the undesired generation of a charge HAP at physiological pH values.

(~ 10) but lethal quantity transition into cross-links [61]. Two competing reactions determine the fate of the initial lesion, progression to cross-links, the rate of which is determined by chemical kinetics, and MGMT mediated repair, the rate of which is determined by the MGMT level. Thus, the sequential delivery of methylating followed by chloroethylating insults can result in profoundly synergistic cytotoxicity due to the efficient MGMT ablation by the low toxicity methylator sensitizing the cells to the far more cytotoxic chloroethylator [62]. Therefore, the use of two similar HAPs independently delivering methylating and chloroethylating cytotoxic stress to HTRs would be expected to be a potent cytotoxic combination to use in conjunction with radiation.

CONCLUSION

Earlier work by our laboratory produced the agent laromustine (1,2-bis(methylsulfonyl)-1-(2-chloroethyl)-2-[(methylamino)carbonyl]hydrazine, also known as cloretazine, onrigin, VNP40101M, 101M). This agent exhibited superior activity to other sulfonylhydrazine prodrugs. This enhanced activity is believed to be the consequence of targeting the higher intracellular pH values (pHi) of cancer cells [63]. Laromustine was activated significantly faster at these higher pH values, releasing a short-lived bis(sulfonyl)hydrazine (1,2-bis(methylsulfonyl)-1-(2-chloroethyl)hydrazine), largely confining its activity to within close proximity of its site of activation and increasing the therapeutic activity. The success of laromustine leads us examining the possibility of using other tumor selective mechanisms to release short-lived bis(sulfonyl)hydrazines and, thus, selectively targeting these tumor markers. We believe that by the exploitation of the tunable short half-lives of bis(sulfonyl)hydrazines, the chemotherapeutic activity can be precisely targeted.

CONSENT FOR PUBLICATION

Not applicable.

FUNDING

This work was supported in part by U.S. Public Health Service Grants CA-090671 and CA-122112 from the National Cancer Institute, and a Grant from the National Foundation for Cancer Research.

CONFLICT OF INTEREST

The authors declare no conflict of interest, financial or otherwise.

ACKNOWLEDGEMENTS

Declared none.

REFERENCES

[1] Dougan, M.; Dranoff, G.; Dougan, S.K. Cancer immunotherapy: beyond checkpoint blockade. *Annual Rev. Cancer Biol.,* **2019**, *3*, 55-75.

[2] Santini, A.; Tenore, G.C.; Novellino, E. Nutraceuticals: a paradigm of proactive medicine. *Eur. J. Pharm. Sci.,* **2017**, *96*, 53-61. http://dx.doi.org/10.1016/j.ejps.2016.09.003 PMID: 27613382

[3] Daliu, P.; Santini, A.; Novellino, E. From pharmaceuticals to nutraceuticals: bridging disease prevention and management. *Expert Rev. Clin. Pharmacol.,* **2019**, *12*(1), 1-7. http://dx.doi.org/10.1080/17512433.2019.1552135 PMID: 30484336

[4] Fang, J.; Nakamura, H.; Maeda, H. The EPR effect: unique features of tumor blood vessels for drug delivery, factors involved, and limitations and augmentation of the effect. *Adv. Drug Deliv. Rev.,* **2011**, *63*(3), 136-151. http://dx.doi.org/10.1016/j.addr.2010.04.009 PMID: 20441782

[5] Awwad, H.K.; Naggar, M.; Mocktar, N.; Barsoum, M. Intercapillary distance measurement as an indicator of hypoxia in carcinoma of the cervix uteri. *Int. J. Radiat. Oncol. Biol. Phys.,* **1986**, *12*(8), 1329-1333. http://dx.doi.org/10.1016/0360-3016(86)90165-3 PMID: 3759554

[6] Leach, R.M.; Treacher, D.F. Oxygen transport-2. Tissue hypoxia. *BMJ,* **1998**, *317*(7169), 1370-1373. http://dx.doi.org/10.1136/bmj.317.7169.1370 PMID: 9812940

[7] Tannock, I.F. Oxygen diffusion and the distribution of cellular radiosensitivity in tumours. *Br. J. Radiol.,* **1972**, *45*(535), 515-524. http://dx.doi.org/10.1259/0007-1285-45-535-515 PMID: 5067983

[8] Wilson, W.R.; Hay, M.P. Targeting hypoxia in cancer therapy. *Nat. Rev. Cancer,* **2011**, *11*(6), 393-410. http://dx.doi.org/10.1038/nrc3064 PMID: 21606941

[9] Braun, R.D.; Lanzen, J.L.; Snyder, S.A.; Dewhirst, M.W. Comparison of tumor and normal tissue oxygen tension measurements using OxyLite or microelectrodes in rodents. *AJP - Heart*, **2001**, pp. 2533-2544.

[10] Brizel, D.M.; Sibley, G.S.; Prosnitz, L.R.; Scher, R.L.; Dewhirst, M.W. Tumor hypoxia adversely affects the prognosis of carcinoma of the head and neck. *Int. J. Radiat. Oncol. Biol. Phys.,* **1997**, *38*(2), 285-289. http://dx.doi.org/10.1016/S0360-3016(97)00101-6 PMID: 9226314

[11] Penketh, P.G.; Shyam, K.; Baumann, R.P.; Ratner, E.S.; Sartorelli, A.C. A simple and inexpensive method to control oxygen concentrations within physiological and neoplastic ranges. *Anal. Biochem.,* **2015**, *491*, 1-3. http://dx.doi.org/10.1016/j.ab.2015.08.032 PMID: 26361820

[12] Pruijn, F.B.; Sturman, J.R.; Liyanage, H.D.; Hicks, K.O.; Hay, M.P.; Wilson, W.R. Extravascular transport of drugs in tumor tissue: effect of lipophilicity on diffusion of tirapazamine analogues in multicellular layer cultures. *J. Med. Chem.,* **2005**, *48*(4), 1079-1087. http://dx.doi.org/10.1021/jm049549p PMID: 15715475

[13] van der Heijden, M.; de Jong, M.C.; Verhagen, C.V.M.; de Roest, R.H.; Sanduleanu, S.; Hoebers, F.; Leemans, C.R.; Brakenhoff, R.H.; Vens, C.; Verheij, M.; van den Brekel, M.W.M. Acute hypoxia profile is a stronger prognostic factor than chronic hypoxia in advanced stage head and neck cancer patients. *Cancers (Basel),* **2019**, *11*(4), 583-596. http://dx.doi.org/10.3390/cancers11040583 PMID: 31027242

[14] Lin, A.J.; Cosby, L.A.; Shansky, C.W.; Sartorelli, A.C. Potential bioreductive alkylating agents. 1. Benzoquinone derivatives. *J. Med. Chem.,* **1972**, *15*(12), 1247-1252. http://dx.doi.org/10.1021/jm00282a011 PMID: 4635968

[15] Sartorelli, A.C. Therapeutic attack of hypoxic cells of solid tumors: presidential address. *Cancer Res.,* **1988**, *48*(4), 775-778. PMID: 3123053

[16] Lin, A.J.; Cosby, L.A.; Sartorelli, A.C. Potential bioreductive alkylating agents. Sartorelli, A.C., Ed.; American Chemical Society: Washington, D.C. *Cancer Chemother*., **1976**, pp. 71-86.

[17] Lin, A.J.; Pardini, R.S.; Cosby, L.A.; Lillis, B.J.; Shansky, C.W.; Sartorelli, A.C. Potential bioreductive alkylating agents. 2. Antitumor effect and biochemical studies of naphthoquinone derivatives. *J. Med. Chem.,* **1973**, *16*(11), 1268-1271. http://dx.doi.org/10.1021/jm00269a010 PMID: 4147836

[18] Le, Q-T.; Denko, N.C.; Giaccia, A.J. Hypoxic gene expression and metastasis. *Cancer Metastasis Rev.,* **2004**, *23*(3-4), 293-310. http://dx.doi.org/10.1023/B:CANC.0000031768.89246.d7 PMID: 15197330

[19] Moulder, J.E.; Rockwell, S. Tumor hypoxia: its impact on cancer therapy. *Cancer Metastasis Rev.,* **1987**, *5*(4), 313-341. http://dx.doi.org/10.1007/BF00055376 PMID: 3552280

[20] Vaupel, P.W.; Frinak, S.; Bicher, H.I. Heterogeneous oxygen partial pressure and pH distribution in C_3H mouse mammary adenocarcinoma. *Cancer Res.,* **1981**, *41*(5), 2008-2013. PMID: 7214369

[21] Minchinton, A.I.; Tannock, I.F. Drug penetration in solid tumours. *Nat. Rev. Cancer,* **2006**, *6*(8), 583-592. http://dx.doi.org/10.1038/nrc1893 PMID: 16862189

[22] Stohrer, M.; Boucher, Y.; Stangassinger, M.; Jain, R.K. Oncotic pressure in solid tumors is elevated. *Cancer Res.,* **2000**, *60*(15), 4251-4255.

PMID: 10945638

[23] Hicks, K.O.; Pruijn, F.B.; Secomb, T.W.; Hay, M.P.; Hsu, R.; Brown, J.M.; Denny, W.A.; Dewhirst, M.W.; Wilson, W.R. Use of three-dimensional tissue cultures to model extravascular transport and predict *in vivo* activity of hypoxia-targeted anticancer drugs. *J. Natl. Cancer Inst.,* **2006**, *98*(16), 1118-1128.
http://dx.doi.org/10.1093/jnci/djj306 PMID: 16912264

[24] Quintiliani, M. Modification of radiation sensitivity: the oxygen effect. *Int. J. Radiat. Oncol. Biol. Phys.,* **1979**, *5*(7), 1069-1076.
http://dx.doi.org/10.1016/0360-3016(79)90621-7 PMID: 389899

[25] Conley, S.J.; Gheordunescu, E.; Kakarala, P.; Newman, B.; Korkaya, H.; Heath, A.N.; Clouthier, S.G.; Wicha, M.S. Antiangiogenic agents increase breast cancer stem cells *via* the generation of tumor hypoxia. *Proc. Natl. Acad. Sci. USA,* **2012**, *109*(8), 2784-2789.
http://dx.doi.org/10.1073/pnas.1018866109 PMID: 22308314

[26] Rasheed, Z.A.; Kowalski, J.; Smith, B.D.; Matsui, W. Concise review: emerging concepts in clinical targeting of cancer stem cells. *Stem Cells,* **2011**, *29*(6), 883-887.
http://dx.doi.org/10.1002/stem.648 PMID: 21509907

[27] Koh, W.J.; Rasey, J.S.; Evans, M.L.; Grierson, J.R.; Lewellen, T.K.; Graham, M.M.; Krohn, K.A.; Griffin, T.W. Imaging of hypoxia in human tumors with [F-18]fluoromisonidazole. *Int. J. Radiat. Oncol. Biol. Phys.,* **1992**, *22*(1), 199-212.
http://dx.doi.org/10.1016/0360-3016(92)91001-4 PMID: 1727119

[28] Brown, J.M. Imaging tumor sensitivity to a bioreductive prodrug: two for the price of one! *Clin. Cancer Res.,* **2012**, *18*(6), 1487-1489.
http://dx.doi.org/10.1158/1078-0432.CCR-11-3267 PMID: 22317761

[29] Riesterer, O.; Honer, M.; Jochum, W.; Oehler, C.; Ametamey, S.; Pruschy, M. Ionizing radiation antagonizes tumor hypoxia induced by antiangiogenic treatment. *Clin. Cancer Res.,* **2006**, *12*(11 Pt 1), 3518-3524.
http://dx.doi.org/10.1158/1078-0432.CCR-05-2816 PMID: 16740778

[30] Kyle, A.H.; Minchinton, A.I. Measurement of delivery and metabolism of tirapazamine to tumour tissue using the multilayered cell culture model. *Cancer Chemother. Pharmacol.,* **1999**, *43*(3), 213-220.
http://dx.doi.org/10.1007/s002800050886 PMID: 9923551

[31] Penketh, P.G.; Shyam, K.; Baumann, R.P.; Ishiguro, K.; Patridge, E.V.; Zhu, R.; Sartorelli, A.C. A strategy for selective O(6)-alkylguanine-DNA alkyltransferase depletion under hypoxic conditions. *Chem. Biol. Drug Des.,* **2012**, *80*(2), 279-290.
http://dx.doi.org/10.1111/j.1747-0285.2012.01401.x PMID: 22553921

[32] Foehrenbacher, A.; Secomb, T.W.; Wilson, W.R.; Hicks, K.O. Design of optimized hypoxia-activated prodrugs using pharmacokinetic/pharmacodynamic modeling. *Front. Oncol.,* **2013**, *3*, 314.
http://dx.doi.org/10.3389/fonc.2013.00314 PMID: 24409417

[33] Shyam, K.; Penketh, P.G.; Baumann, R.P.; Finch, R.A.; Zhu, R.; Zhu, Y.L.; Sartorelli, A.C. Antitumor sulfonylhydrazines: design, structure-activity relationships, resistance mechanisms, and strategies for improving therapeutic utility. *J. Med. Chem.,* **2015**, *58*(9), 3639-3671.
http://dx.doi.org/10.1021/jm501459c PMID: 25612194

[34] Penketh, P.G.; Shyam, K.; Sartorelli, A.C. Studies on the mechanism of decomposition and structural factors affecting the aqueous stability of 1,2-bis(sulfonyl)-1-alkylhydrazines. *J. Med. Chem.,* **1994**, *37*(18), 2912-2917.
http://dx.doi.org/10.1021/jm00044a012 PMID: 8071939

[35] Webb, B.A.; Chimenti, M.; Jacobson, M.P.; Barber, D.L. Dysregulated pH: a perfect storm for cancer progression. *Nat. Rev. Cancer,* **2011**, *11*(9), 671-677.
http://dx.doi.org/10.1038/nrc3110 PMID: 21833026

[36] Ishiguro, K.; Zhu, Y-L.; Shyam, K.; Penketh, P.G.; Baumann, R.P.; Sartorelli, A.C. Quantitative relationship between guanine O(6)-alkyl lesions produced by Onrigin™ and tumor resistance by O(6)-alkylguanine-DNA alkyltransferase. *Biochem. Pharmacol.,* **2010**, *80*(9), 1317-1325.
http://dx.doi.org/10.1016/j.bcp.2010.07.022 PMID: 20654586

[37] Baumann, R.P.; Penketh, P.G.; Ishiguro, K.; Shyam, K.; Zhu, Y.L.; Sartorelli, A.C. Reductive activation of the prodrug 1,2-bis(methylsulfonyl)-1-(2-chloroethyl)-2-[[1-(4-nitrophenyl)ethoxy]carbonyl]hydrazine (KS119) selectively occurs in oxygen-deficient cells and overcomes O(6)-alkylguanine-DNA alkyltransferase mediated KS119 tumor cell resistance. *Biochem. Pharmacol.,* **2010**, *79*(11), 1553-1561.
http://dx.doi.org/10.1016/j.bcp.2009.12.004 PMID: 20005211

[38] Ishiguro, K.; Shyam, K.; Penketh, P.G.; Sartorelli, A.C. Development of an O(6)-alkylguanine-DNA alkyltransferase assay based on covalent transfer of the benzyl moiety from [benzene-3H]O(6)-benzylguanine to the protein. *Anal. Biochem.,* **2008**, *383*(1), 44-51.
http://dx.doi.org/10.1016/j.ab.2008.08.009 PMID: 18783719

[39] Citron, M.; Decker, R.; Chen, S.; Schneider, S.; Graver, M.; Kleynerman, L.; Kahn, L.B.; White, A.; Schoenhaus, M.; Yarosh, D. O6-methylguanine-DNA methyltransferase in human normal and tumor tissue from brain, lung, and ovary. *Cancer Res.,* **1991**, *51*(16), 4131-4134.
PMID: 1868433

[40] Christmann, M.; Verbeek, B.; Roos, W.P.; Kaina, B. O(6)-Methylguanine-DNA methyltransferase (MGMT) in normal tissues and tumors: enzyme activity, promoter methylation and immunohistochemistry. *Biochim. Biophys. Acta,* **2011**, *1816*(2), 179-190.
PMID: 21745538

[41] Zhu, R.; Liu, M.C.; Luo, M.Z.; Penketh, P.G.; Baumann, R.P.; Shyam, K.; Sartorelli, A.C. 4-nitrobenzyloxycarbonyl derivatives of O(6)-benzylguanine as hypoxia-activated prodrug inhibitors of O(6)-alkylguanine-DNA alkyltransferase (AGT), which produces resistance to agents targeting the O-6 position of DNA guanine. *J. Med. Chem.,* **2011**, *54*(21), 7720-7728.
http://dx.doi.org/10.1021/jm201115f PMID: 21955333

[42] Baumann, R.P.; Seow, H.A.; Shyam, K.; Penketh, P.G.; Sartorelli, A.C. The antineoplastic efficacy of the prodrug Cloretazine is produced by the synergistic interaction of carbamoylating and alkylating products of its activation. *Oncol. Res.,* **2005**, *15*(6), 313-325.
http://dx.doi.org/10.3727/096504005776404553 PMID: 16408696

[43] Shyam, K.; Penketh, P.G.; Shapiro, M.; Belcourt, M.F.; Loomis, R.H.; Rockwell, S.; Sartorelli, A.C. Hypoxia-selective nitrobenzyloxycarbonyl derivatives of 1,2-bis(methylsulfonyl)-1-(2-chloroethyl)hydrazines. *J. Med. Chem.,* **1999**, *42*(5), 941-946.
http://dx.doi.org/10.1021/jm9805891 PMID: 10072691

[44] Seow, H.A.; Penketh, P.G.; Shyam, K.; Rockwell, S.; Sartorelli, A.C. 1,2-Bis(methylsulfonyl)-1-(2-chloroethyl)-2-[[1-(4-nitrophenyl)ethoxy]carbonyl]hydrazine: an anticancer agent targeting hypoxic cells *Proc Natl Acad Sc.,* **2005**, *102*, 9282-7.

[45] Penketh, P.G.; Baumann, R.P.; Shyam, K.; Williamson, H.S.; Ishiguro, K.; Zhu, R.; Eriksson, E.S.; Eriksson, L.A.; Sartorelli, A.C. 1,2-Bis(methylsulfonyl)-1-(2-chloroethyl)-2-[[1-(4-nitrophenyl)ethoxy]carbonyl]hydrazine (KS119): a cytotoxic prodrug with two stable conformations differing in biological and physical properties. *Chem. Biol. Drug Des.,* **2011**, *78*(4), 513-526.
http://dx.doi.org/10.1111/j.1747-0285.2011.01193.x PMID: 21777394

[46] Zhu, R.; Seow, H.A.; Baumann, R.P.; Ishiguro, K.; Penketh, P.G.; Shyam, K.; Sartorelli, A.C. Design of a hypoxia-activated prodrug inhibitor of O6-alkylguanine-DNA alkyltransferase. *Bioorg. Med. Chem. Lett.,* **2012**, *22*(19), 6242-6247.
http://dx.doi.org/10.1016/j.bmcl.2012.08.008 PMID: 22932317

[47] Grunbein, W.; Fojtik, A.; Henglein, A. Pulsradiolytische Bestimmung der Absorptions-spektren und Dissoziationskonstanten kurzlebiger halbreduzierter aromatischer Nitroverbindungen. *Z. Naturforsch. B,* **1969**, *24b*, 1336-1338.
http://dx.doi.org/10.1515/znb-1969-1024

[48] Einstein, A. On the motion of small particles suspended in liquids at rest required by the molecular-kinetic theory of heat. *Ann. Phys.,* **1905**, *17*, 549-560.
http://dx.doi.org/10.1002/andp.19053220806

[49] Wardman, P. Reduction potentials of one-electron couples involving free radicals in aqueous solutions. *J. Phys. Chem. Data,* **1989**, *18*, 1637-1754.
http://dx.doi.org/10.1063/1.555843

[50] Wardman, P. The importance of radiation chemistry to radiation and free radical biology (The 2008 Silvanus Thompson Memorial Lecture). *Br. J. Radiol.,* **2009**, *82*(974), 89-104.
http://dx.doi.org/10.1259/bjr/60186130 PMID: 19168690

[51] Wardman, P. Some reactions and properties of nitro radical-anions important in biology and medicine. *Environ. Health Perspect.,* **1985**, *64*, 309-320.
http://dx.doi.org/10.1289/ehp.8564309 PMID: 3830700

[52] Rajapakse, A.; Linder, C.; Morrison, R.D.; Sarkar, U.; Leigh, N.D.; Barnes, C.L.; Daniels, J.S.; Gates, K.S. Enzymatic conversion of 6-nitroquinoline to the fluorophore 6-aminoquinoline selectively under hypoxic conditions. *Chem. Res. Toxicol.,* **2013**, *26*(4), 555-563.

http://dx.doi.org/10.1021/tx300483z PMID: 23488987

[53] Kim, E.Y.; Liu, Y.; Akintujoye, O.M.; Shyam, K.; Grove, T.A.; Sartorelli, A.C.; Rockwell, S. Preliminary studies with a new hypoxia-selective cytotoxin, KS119W, *in vitro* and *in vivo*. *Radiat. Res.,* **2012**, *178*(3), 126-137.
http://dx.doi.org/10.1667/RR2934.1 PMID: 22862779

[54] Stanford, A.L. Foundations of biophysics. *Elsevier, Academic New York USA*, **1975**, pp. 404.

[55] Lancaster, J.R. Jr. Simulation of the diffusion and reaction of endogenously produced nitric oxide. *Proc. Natl. Acad. Sci. USA,* **1994**, *91*(17), 8137-8141.
http://dx.doi.org/10.1073/pnas.91.17.8137 PMID: 8058769

[56] Hobbie, R.K. Intermediate physics for medicine and biology. Wiley Press, **1978**, pp. 505**.**

[57] Crooks, J.E. Measurement of diffusion coefficients. *J. Chem. Educ.,* **1989**, *66*, 614-615.
http://dx.doi.org/10.1021/ed066p614

[58] Kimura, H.; Braun, R.D.; Ong, E.T.; Hsu, R.; Secomb, T.W.; Papahadjopoulos, D.; Hong, K.; Dewhirst, M.W. Fluctuations in red cell flux in tumor microvessels can lead to transient hypoxia and reoxygenation in tumor parenchyma. *Cancer Res.,* **1996**, *56*(23), 5522-5528.
PMID: 8968110

[59] Shyam, K.; Penketh, P.G.; Loomis, R.H.; Sartorelli, A.C. Thiolysable prodrugs of 1,2-bis(methylsulfonyl)-1-(2-chloroethyl) hydrazine with antineoplastic activity. *Eur. J. Med. Chem.,* **1998**, *33*, 609-615.
http://dx.doi.org/10.1016/S0223-5234(98)80019-6

[60] Rasouli-Nia, A.; Sibghat-Ullah, ; Mirzayans, R.; Paterson, M.C.; Day, R.S., III On the quantitative relationship between O6-methylguanine residues in genomic DNA and production of sister-chromatid exchanges, mutations and lethal events in a Mer- human tumor cell line. *Mutat. Res.,* **1994**, *314*(2), 99-113.
http://dx.doi.org/10.1016/0921-8777(94)90074-4 PMID: 7510369

[61] Penketh, P.G.; Baumann, R.P.; Ishiguro, K.; Shyam, K.; Seow, H.A.; Sartorelli, A.C. Lethality to leukemia cell lines of DNA interstrand cross-links generated by Cloretazine derived alkylating species. *Leuk. Res.,* **2008**, *32*(10), 1546-1553.
http://dx.doi.org/10.1016/j.leukres.2008.03.005 PMID: 18479747

[62] Zhu, R.; Baumann, R.P.; Patridge, E.; Penketh, P.G.; Shyam, K.; Ishiguro, K.; Sartorelli, A.C. Chloroethylating and methylating dual function antineoplastic agents display superior cytotoxicity against repair proficient tumor cells. *Bioorg. Med. Chem. Lett.,* **2013**, *23*(6), 1853-1859.
http://dx.doi.org/10.1016/j.bmcl.2013.01.016 PMID: 23395657

[63] Penketh, P.G.; Finch, R.A.; Sauro, R.; Baumann, R.P.; Ratner, E.S.; Shyam, K. pH-dependent general base catalyzed activation rather than isocyanate liberation may explain the superior anticancer efficacy of laromustine compared to related 1,2-bis(methylsulfonyl)-1-(2-chloroethyl)hydrazine prodrugs. *Chem. Biol. Drug Des.,* **2018**, *91*(1), 62-74.
http://dx.doi.org/10.1111/cbdd.13057 PMID: 28636806